


## Research Paper

# Dual-objective optimization of photovoltaic and electrolyzer size ratios for hydrogen production: economic and carbon emissions perspectives

Francesco Guarino, Angelo Gucciardi, Fabio Massaro, Francesco Montana, Salvatore Ruffino<sup>\*</sup> 

Department of Engineering, University of Palermo, Palermo, Italy

## ARTICLE INFO

## Keywords:

Electrolyzer  
Energy hub  
Green hydrogen  
Optimization  
Photovoltaic

## ABSTRACT

Hydrogen is a zero-emissions fuel that, if generated from renewable energy sources, can play a vital role in reducing carbon emissions across multiple sectors. Green hydrogen production plants are constrained by the availability of renewable sources and there is not a common sizing criterion to couple water electrolyzers with renewable technologies. This study aims at filling the research gap involving the preliminary sizing of water electrolyzers to be coupled with photovoltaic systems according to different objectives and final production targets. The problem was formulated and addressed using a MILP optimization algorithm in MATLAB and solved according to the minimum costs and minimum carbon emissions criteria. Additionally, the optimization algorithm was run on three different final demand scenarios: hydrogen production from stand-alone plant, production to meet hydrogen final demand, and production to meet hydrogen and electricity final demands. Results show that the optimal ratio is between about 1.8 and 2 in the cases with cost minimization, but it increases up to 5.75 when both costs and carbon emissions are taken into account.

## 1. Introduction

### 1.1. Motivation

The ongoing global energy transition, characterized by the large-scale integration of renewable energy sources into final energy consumption, is a critical strategy in mitigating climate change and reducing dependence on fossil fuels. As nations strive to meet the targets set by the Paris Agreement and achieve net-zero emissions by mid-century, the decarbonization of energy systems has become a paramount objective. Among the various clean energy solutions, hydrogen—particularly green hydrogen—has emerged as a key enabler of this transition due to its versatility, high energy density, and potential to decarbonize traditionally hard-to-abate sectors such as heavy industry, long-haul transportation, and chemical production.

Hydrogen possesses several intrinsic advantages that make it a compelling energy vector. With an energy density of 120 MJ/kg [1], it far surpasses conventional fossil fuels on a mass basis, making it ideal for applications requiring high energy storage capacity. Additionally, hydrogen is the most abundant element in the universe, ensuring its long-term availability as a resource. Unlike fossil fuels, its combustion or

electrochemical conversion in fuel cells produces only water vapor, eliminating direct CO<sub>2</sub> emissions. These attributes position hydrogen as a critical component in future sustainable energy systems, capable of serving multiple roles—including power generation (via fuel cells or hydrogen turbines), heat production (in industrial boilers and cogeneration systems), and as a feedstock for synthetic fuels and chemicals.

However, despite its advantages, hydrogen faces significant challenges that hinder its widespread adoption. The most pressing issue is its high production cost, primarily because hydrogen does not naturally occur in its pure form and must be extracted from other compounds, such as water or hydrocarbons. Currently, the hydrogen market is dominated by “gray hydrogen”, which is produced via steam methane reforming (SMR) of natural gas—a process that emits 9–12 kg of CO<sub>2</sub> per kg of hydrogen. A marginally cleaner alternative is “blue hydrogen”, which employs Carbon Capture and Storage (CCS) to mitigate emissions from SMR, though it still relies on fossil fuels and suffers from CCS inefficiencies and leakage risks.

In contrast, “green hydrogen”, produced through water electrolysis powered by renewable electricity (e.g., solar PV or wind), offers a truly sustainable pathway with near-zero carbon emissions. Yet, despite its environmental benefits, green hydrogen remains 2–4 times more expensive than gray hydrogen, primarily due to the high capital and

<sup>\*</sup> Corresponding author.

E-mail address: [salvatore.ruffino07@unipa.it](mailto:salvatore.ruffino07@unipa.it) (S. Ruffino).

| Nomenclature         |  | Symbols              |                         |
|----------------------|--|----------------------|-------------------------|
| <i>Abbreviations</i> |  | <i>C</i>             | Cost                    |
| CCS                  | Carbon Capture and Storage                       | <i>R</i>             | Revenue                 |
| CRF                  | Capital Recovery Factor                          | <i>A</i>             | Area                    |
| EES                  | Electrical Energy Storage                        | <i>DoD</i>           | Depth of Discharge      |
| EL                   | Electrolyzer                                     | <i>E</i>             | Electricity             |
| ETHOS                | Energy Transformation PatHway Optimization Suite | <i>H<sub>2</sub></i> | Hydrogen                |
| GWP                  | Global Warming Potential                         | <i>n</i>             | Useful life             |
| H2SS                 | Hydrogen Storage System                          | <i>K</i>             | Efficiency              |
| LCOE                 | Levelized Cost Of Electricity                    | $\beta$              | Temperature coefficient |
| LCOH                 | Levelized Cost Of Hydrogen                       | <i>S</i>             | rated Size              |
| MILP                 | Mixed-Integer Linear Programming                 | <i>SOC</i>           | State Of Charge         |
| MOOP                 | Multi-Objective Optimization Problem             | <i>W</i>             | Water                   |
| NOCT                 | Nominal Operating Cell Temperature               | <i>Subscripts</i>    |                         |
| PEM                  | Polymer Electrolyte Membrane                     | <i>CAPEX</i>         | CAPital EXpenditure     |
| PV                   | PhotoVoltaic                                     | <i>day</i>           | Day of the year         |
| RES                  | Renewable Energy Source                          | <i>dem</i>           | Demand                  |
| SMR                  | Steam Methane Reforming                          | <i>in</i>            | Inlet flow              |
| TR                   | TRansformer                                      | <i>OPEX</i>          | OPerating EXpenditure   |
| WT                   | Wind Turbine                                     | <i>out</i>           | Outlet flow             |
|                      |  | <i>year</i>          | Standard year           |

operational costs of electrolyzers and the intermittent nature of renewable energy sources. According to the International Energy Agency (IEA), green hydrogen accounted for less than 0.1 % of global hydrogen production in 2023, with projections indicating it will only reach 4 % by 2030 under current policies [2]. This slow uptake is attributed to low demand in emerging sectors, high production costs, and insufficient infrastructure for storage and distribution.

Hydrogen demand to date remains concentrated in refining and industrial applications where hydrogen has been already used for decades. Its adoption in new applications where hydrogen is expected to play a key role in the transition to clean energy, such as heavy industry and long- distance transportation, accounts for less than 1% of global demand [3].

Focusing on green hydrogen, namely hydrogen produced from water electrolysis using renewable electricity, its current global diffusion is growing although it was still below 100 kton in 2023 [3]. With the diffusion of this new technology, several studies were developed in scientific and technical literature, analyzing the possible benefits of introducing electrolyzers close to large wind or solar farms.

## 1.2. Literature review

Proper design of a clean hydrogen production facility is critical to the cost of the final product and, therefore, to foster growth in demand for this energy carrier. With respect to the plant layout, three main coupling configurations can be found in literature:

- Coupling through energy storage configuration, with renewable systems charging the storage system that is used to buffer the intermittency of renewable energy (usually solar or wind). Batteries store excess energy during peak production and supply it to the electrolyzer during low generation periods. Nevertheless, the costs for the battery should carefully be balanced against its benefits;
- Direct coupling configuration, where the renewable system energy production is directly fed to the electrolyzer without additional intermediate components. While this configuration reduces capital costs with respect to the previous solution, it suffers from reduced capacity factors due to the solar irradiance variations;

- Hybrid systems, integrating several renewable energy sources or grid connections. Such configurations enhance reliability and optimize hydrogen production by diversifying energy inputs.

The relationship between the rated size of the renewable power plant and the size of the electrolyzer to be fed is among the main design parameters to assess in such plants. In detail, it is well known that intermittent renewable energies have a large variability over the day and over the year, thus the peak power production occurs a few hours per year, especially for photovoltaic systems. This might suggest reducing the rated size of the water electrolyzer. On the opposite, an excessive downsizing might cause an unnecessary reduction of the green hydrogen production. In addition, large scale plants might face problems related to the soil occupation. For what above, identifying a criterion for the ratio between the rated size of the renewable system and the one of electrolyzer is crucial and, although the popularity of green hydrogen production in recent scientific literature, this problem was rarely assessed in an explicit manner.

The report [3] summarizes the optimal values of this ratio for different world regions, calculated with the Energy Transformation PatHway Optimization Suite (ETHOS) model [4]. In this study, the optimal ratio is the value that minimizes the levelized cost of hydrogen (LCOH) [5]. According to this study, with respect to electricity production from photovoltaics (PV), the optimal ratio between the rated sizes is between 1.3 and 1.7 in locations with excellent solar irradiation availability, such as Africa, Chile, and the Middle East, while it takes a value of 2 in Europe. However, the optimization model did not take into account for the use of the renewable electricity produced by the same plant for other purposes besides the production of green hydrogen.

In [6], the author presented a multi-objective optimization study for sizing a decentralized small- scale plant consisting of wind turbines, batteries, power converters, alkaline electrolyzer and hydrogen tank. The optimization objective functions are the maximum hydrogen demand coverage, the minimum LCOH, minimum energy dump possibility, minimum carbon dioxide emissions and maximization of natural gas preserved. The results of this study show that, to fully meet the hydrogen demand, the wind power capacity should be 3.43 times higher than the one of the electrolyzer, also including a battery and a hydrogen tank in the system. This integrated wind- hydrogen system would allow avoiding 87.75 tons per year of CO<sub>2</sub> emissions but with a really high LCOH of

**Table 1**  
Main features of the studies reported in the literature review.

| Ref.       | Renewable energy system                                 | Objective functions  | Other uses of renewable electricity | Optimal ratio RES/EL   |
|------------|---|--|-------------------------------------|--|
| [3,4]      | PV systems, onshore wind turbines (WT)                  | LCOH minimization  | No                                  | 1.3-2.4 for PV/EL<br>1-2.8 for WT/EL                                 |
| [6]        | Wind turbines   | Maximum hydrogen demand coverage, minimum LCOH, minimum energy dump possibility, minimum carbon dioxide emissions and maximization of natural gas preserved  | No                                  | 3.43   |
| [7]        | PV systems  | Costs minimization   | Yes                                 | 1-7.7  |
| [10]       | PV systems-only, wind turbines-only, and hybrid PV-wind | LCOH minimization for cases where electrolyzers are powered by PV systems-only and wind turbines-only; hydrogen production maximization and energy transfer to and from the grid minimization for hybrid PV- wind case | No                                  | 1.7 for PV-only/EL<br>2.5 for WT-only/EL<br>1.63 for hybrid PV-WT/EL |
| [11]       | Hybrid PV-wind systems                                  | Minimization of LCOE and maximization of capacity factor and full-load operating hours of the electrolyzer   | No                                  | 2.35-4.58  |
| This study | PV systems  | Minimization of costs and carbon emissions   | Yes                                 | 1.8-5.75   |

33.70 \$/kg (about 31 €/kg).

In [7], a particle swarm optimization algorithm was presented for the design and operation of an autonomous microgrid with electrical and hydrogen loads, with the goal of minimizing costs. The optimal design of the microgrid involves an oversized PV system and high potential energy wastage, showing that oversizing the PV system is cheaper than increasing the energy storage with an appropriately sized solar system. Similar results were obtained in the study reported in [8], where the authors showed that, although batteries affect only 5–6 % of the operating and investment expenses for a renewable hydrogen production plant from PV, their presence results in a higher LCOH, so it is more cost-effective to sell the excess energy produced by PV to the grid than to store it to increase hydrogen production. The same conclusion was reached by the study reported in [9], where a hybrid wind/photovoltaic system was analyzed to power the electrolyzer.

In [10], the authors presented two optimization cases: the first one aims at the optimal sizing of a system consisting of PEM electrolyzer, photovoltaic and/or wind power system, with the purpose of minimizing LCOH, showing how hydrogen production based on wind power is more cost-effective than production from photovoltaic systems; the second one, on the other hand, aims at finding the optimal ratio between photovoltaic and wind power capacity to maximize hydrogen production and minimize energy transfer to and from the grid. Environmental aspects such as carbon emissions were therefore not analyzed.

In [11], a techno-economic optimization case for sizing a photovoltaic-wind hybrid system to power an electrolysis plant was presented, with the objective of finding a trade-off between minimizing the levelized cost of energy (LCOE) and maximizing the capacity factor and full-load operating hours of the electrolyzer. Specifically, the size of the PV system was fixed, while the size of the wind farm was varied to find the optimal configuration that, integrated with the PV system, produces the best results. Again, the environmental aspect related to carbon emissions was neglected.

In the study reported in [12], on the other hand, a comparison was made between the direct and indirect configuration for the electrical coupling between the photovoltaic system and the electrolyzer, but without indicating a procedure for their optimal sizing.

Finally, although photovoltaic and wind are the most common renewable energy systems, some authors also proposed coupling electrolyzers with other technologies. For example, in [13], the authors propose a concept of wave energy converter for onshore application (harbors, breakwaters, etc.) to be coupled with an alkaline electrolyzer. The simulations show that the converter might produce about 10 MWh/year, with a resulting 2000 m<sup>3</sup>/year of green hydrogen production. The authors propose to store green hydrogen and convert it into electricity into a fuel cell when the power grid allows the injection of additional energy.

A summary of the studies described in this literature review section is given in Table 1.

### 1.3. Contribution

This article focuses on explicitly illustrate a sizing method for the renewable electricity production system and the water electrolyzer in a green hydrogen production plant. In order to identify the best techno-economic possibility, this study adopts an optimization model to assess the possible combinations of rated size between these two components, maximizing the overall performance of the system in terms of economic feasibility and the life-cycle CO<sub>2</sub> emissions. This paper aims to find this optimal ratio by examining the problem considering three distinct scenarios:

- Scenario 1: no demand for hydrogen or electricity, the energy carriers produced are sold to external markets.
- Scenario 2: industrial hydrogen demand, no demand for electricity, allowing the sale of excess production of energy carriers.

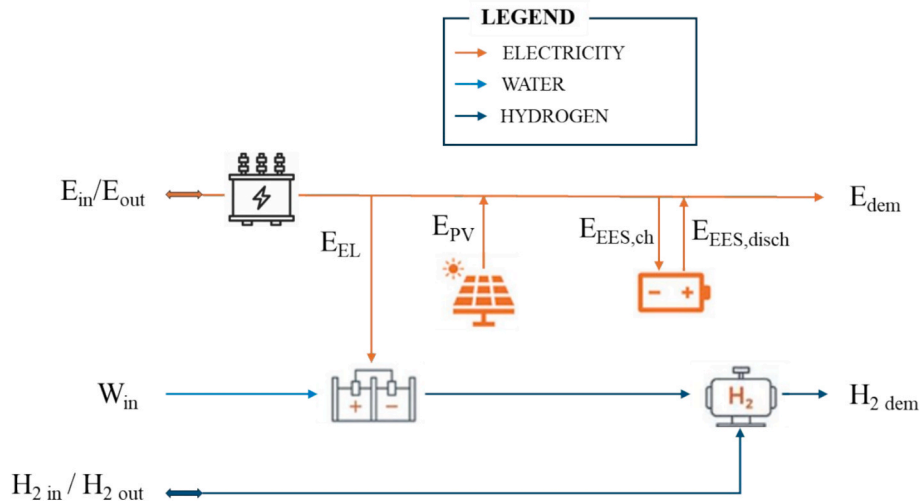


Fig. 1. Schematic of the energy hub model.

**Table 2**  
Coefficients used for the economic objective function.

| Coefficient    | Meaning                                      | Value  |
|----------------|--|--|
| $Copex, E$     | Electricity purchase price                   | 0.1218 €/kWh [23]  |
| $Copex, W$     | Water purchase price                         | 4.16 [14]  |
| $Copex, H2$    | Hydrogen purchase price                      | 12.89 €/kg [14]  |
| $Ropex, E$     | Electricity sell price                       | 0.05 €/kWh [24]  |
| $Ropex, H2$    | Green hydrogen sell price                    | 10 €/kg  |
| $Ccapex, PV$   | Investment cost for PV system                | 779.95 €/kW [25]   |
| $Ccapex, EES$  | Investment cost for EES system               | 259.35 €/kWh [25]  |
| $Ccapex, EL$   | Investment cost for EL                       | 753.48 €/kW (average from [6 26])                                    |
| $Ccapex, H2SS$ | Investment cost for H2SS                     | 904.72 €/kg H <sub>2</sub> (average from [6])                        |
| $Copex, PV$    | Operation and maintenance cost for PV system | 7.505 €/(kW year) [25]   |
| $Copex, EL$    | Operation and maintenance cost for EL        | 15.07 €/(kW year) [26]   |
| $i$            | Interest rate for CRF calculation            | 6 % (equal to the WACC in the distribution and metering sector [27]) |

**Table 3**  
Coefficients used for the emission objective function.

| Coefficient | Meaning   | Value  |
|-------------|---|--|
| $GWPE$      | Global warming potential of electricity from the grid | 0.7089 kg CO <sub>2,eq</sub> /kWh [28]                                   |
| $GWPW$      | Global warming potential of purchased water           | 0 kg CO <sub>2,eq</sub> /m <sup>3</sup> (negligible)                     |
| $GWPH2$     | Global warming potential of purchased hydrogen        | 1.5500 kg CO <sub>2,eq</sub> /kg H <sub>2</sub> (average value from [3]) |
| $GWPPV$     | Global warming potential of PV system                 | 357.732 kg CO <sub>2,eq</sub> /kWp                                       |
| $GWPEES$    | Global warming potential of EES system                | 76.284 kg CO <sub>2,eq</sub> /kWh  |
| $GWPEL$     | Global warming potential of EL                        | 28.000 kg CO <sub>2,eq</sub> /kW   |
| $GWPH2SS$   | Global warming potential of H2SS                      | 0.048 kg CO <sub>2,eq</sub> /kg H <sub>2</sub>                           |
| $nPV$       | Useful lifetime of PV system                          | 25 years   |
| $nEES$      | Useful lifetime of EES system                         | 8 years  |
| $nEL$       | Useful lifetime of EL                                 | 15 years   |
| $nH2SS$     | Useful lifetime of H2SS                               | 12 years   |

- Scenario 3: industrial hydrogen and electricity demand, allowing the sale of excess production of energy carriers.

A Mixed-Integer Linear Programming (MILP) energy hub optimization model was developed to carry out the multi-objective optimization

**Table 4**  
Additional technical parameters for the case study.

| Coefficient  | Meaning  | Value   |
|--------------|--|---|
| $KTR$        | Electrical transformer efficiency                    | 0.98  |
| $Edem$       | Electricity final demand                             | 500 MWh/h [14]                                    |
| $H2 dem$     | Hydrogen final demand                                | 7212.3 kg/h [14]                                  |
| $KEES,loss$  | Battery self-discharge rate                          | 0.01 h <sup>-1</sup> [29]                         |
| $KEES,ch$    | Battery charge efficiency                            | 0.97  |
| $KEES,dich$  | Battery discharge efficiency                         | 0.97  |
| $KH2SS,loss$ | Hydrogen tank self-discharge rate                    | 0.02 h <sup>-1</sup> [29]                         |
| $KH2SS,ch$   | Hydrogen tank charge efficiency                      | 0.99  |
| $KH2SS,dich$ | Hydrogen tank discharge efficiency                   | 0.99  |
| $APV$        | PV module area                                       | 1.6368 m <sup>2</sup>                             |
| $KPV$        | PV average radiation to electricity efficiency       | 0.1625 (including losses in the balance of plant) |
| $\beta PV$   | PV cell temperature coefficient                      | -2.75•10 <sup>-3</sup> °C <sup>-1</sup>           |
| $GNOCT$      | Reference solar radiation                            | 800 W/m <sup>2</sup>                              |
| $NOCT$       | PV nominal operating cell temperature                | 45 °C   |
| $Ta,NOCT$    | Reference air temperature                            | 20 °C   |
| $Tref$       | Reference cell temperature                           | 25 °C   |
| $SPVm$       | Rated power of a single photovoltaic module          | 0.4 kW  |
| $SEES,max$   | Maximum allowed battery capacity                     | 1•10 <sup>7</sup> kWh                             |
| $DoDEES$     | Battery depth of discharge rate                      | 0.2   |
| $KEL,eh2$    | Electrolyzer electricity to hydrogen production rate | 0.02 kg/kWh                                       |
| $KEL,wh2$    | Electrolyzer water to hydrogen conversion rate       | 0.1 kg/L  |
| $SH2SS,max$  | Maximum allowed hydrogen tank capacity               | 1•10 <sup>7</sup> kg                              |
| $DoDH2SS$    | Hydrogen tank depth of discharge rate                | 0.1   |

**Table 5**  
Optimal rated sizes, annualized costs and annualized carbon emissions for the economic optimization studies.

| Component                                      | Scenario 1    | Scenario 2  | Scenario 3  |
|--|---------------|-------------|-------------|
| PV system [MWp]                                | 55.1          | 55.1        | 55.1        |
| EL [MW]  | 0             | 29.7        | 27.1        |
| EES [MWh]                                      | 0             | 0           | 0           |
| H2SS [ton H2]                                  | 8.2           | 8.2         | 0.6         |
| <b>PV/EL ratio</b>                             | -             | 1.85        | 2.03        |
| <b>Annualized Costs [€]</b>                    | 2,075,896,576 | 673,335,241 | -5,159,988  |
| <b>Annualized Carbon Emissions [kg CO2,eq]</b> | 3,709,769,322 | 619,051,934 | -16,374,280 |

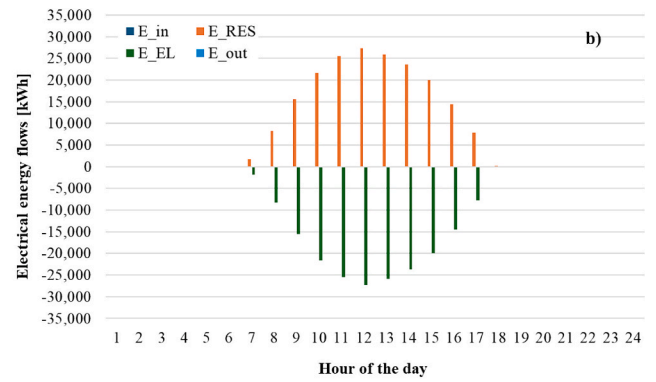
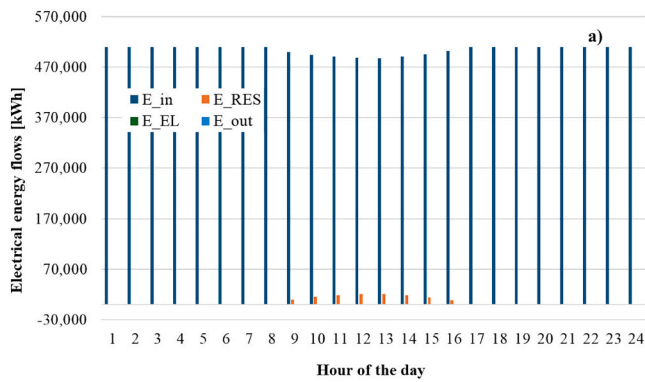


Fig. 2. Example of electrical energy flows daily trend in economic minimization studies. a) Scenario 1; b) Scenarios 2 and 3.

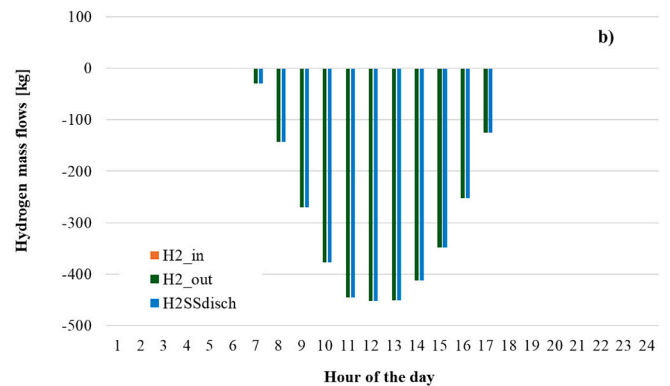
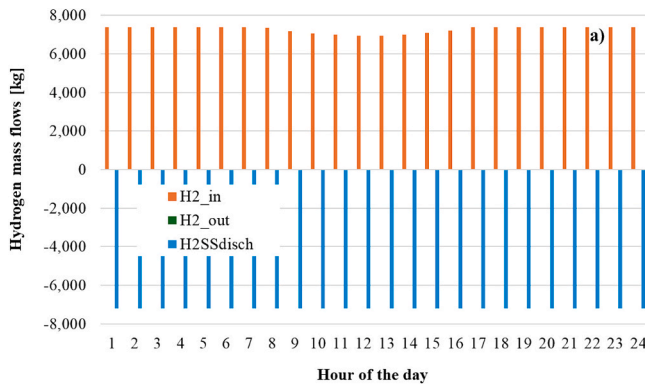


Fig. 3. Example of hydrogen mass flows daily trend in economic minimization studies. a) Scenarios 1 and 2; b) Scenario 3.

Table 6

Optimal rated sizes, annualized costs and annualized carbon emissions for the environmental optimization studies.

| Component  | Scenario 1    | Scenario 2  | Scenario 3  |
|--|---------------|-------------|-------------|
| PV system [MWp]                                      | 55.1          | 55.1        | 55.1        |
| EL [MW]  | 0             | 0           | 0           |
| EES [MWh]  | 0             | 0           | 0           |
| H2SS [ton H2]  | 8.2           | 8.2         | 0           |
| PV/EL ratio  | -             | -           | -           |
| Annualized Costs [€]                                 | 2,076,384,821 | 680,156,783 | -369,881    |
| Annualized Carbon Emissions [kg CO <sub>2</sub> ,eq] | 3,709,769,322 | 585,836,514 | -48,904,458 |

aimed at minimizing the total costs and the life-cycle CO<sub>2</sub> emissions of the system. Thanks to this approach, the study provides insight into the trade-offs between economic performance and the contribution to greenhouse effect under different demand conditions. The mathematical model adopted is a generic model that can be used for various applications, such as single residential systems or small community systems. However, this study focuses on industrial contexts, where, given the size of the plants, benefits such as economies of scale and higher conversion efficiencies can be obtained.

Among Renewable Energy Sources (RES), PV technology was selected for this study due to its widespread availability, scalability, and declining costs. Nevertheless, the mathematical model can be easily modified in order to include different or additional RES technologies.

This study enriches a previous article carried out by some of the authors [14], in which an economic optimization was made on an

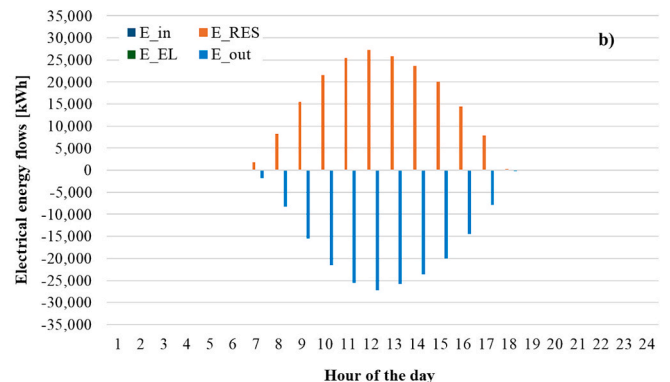
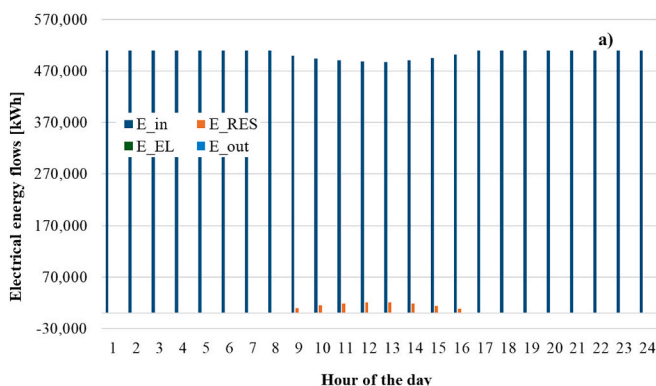


Fig. 4. Example of electrical energy flows daily trend in emissions minimization studies. a) Scenario 1; b) Scenarios 2 and 3.

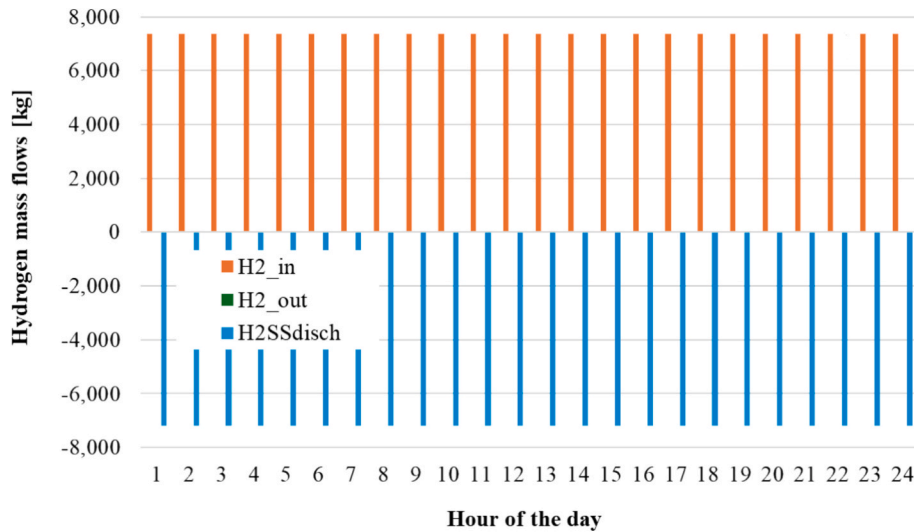


Fig. 5. Example of hydrogen mass flows daily trend in emissions minimization studies - Scenarios 1 and 2 (hydrogen flows are not involved in optimal Scenario 3).

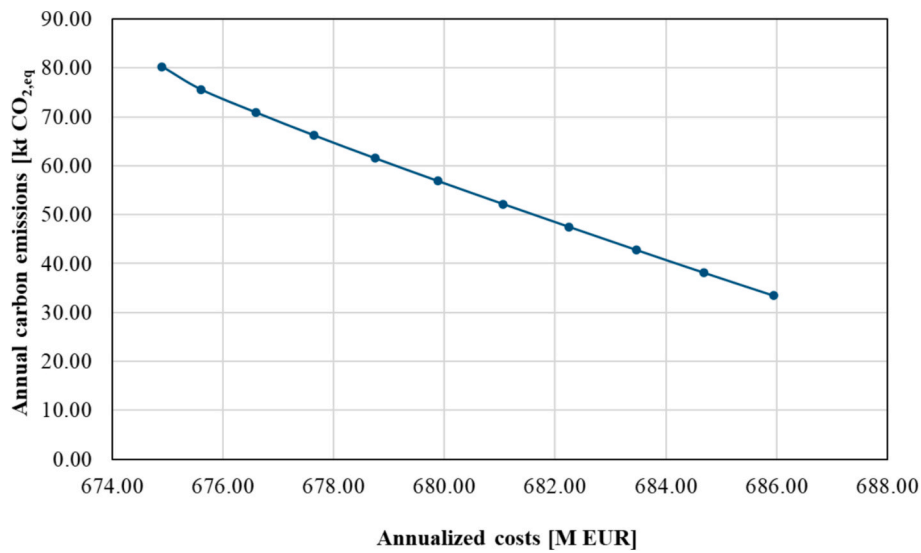


Fig. 6. Pareto front for the scenario 2.

industrial facility having both electricity and hydrogen demands, although in that case selling the excess energy carriers outside the hub was prevented. It is important to highlight that, although this study and this mathematical model were specifically conceived to simulate the coupling of water electrolyzers and photovoltaic systems, all the equations are generic balances and this model might be easily extended to different renewable energies, as specified in subsequent sections.

This paper is structured as follows: in Section 2, the energy hub model and the equations used to solve the problem are described. The case studies are described in Section 3, while the results of the simulations carried out for this paper are illustrated in Section 4. Last, the conclusions of the study are provided in Section 5.

## 2. Materials and methods

### 2.1. Modelling approach

In order to identify the optimal coupling of rated sizes between photovoltaic system and water electrolyzer, a MILP energy hub multi-objective optimization model was developed. The schematic of the energy hub model studied in this paper is shown in Fig. 1.

The energy hub modeling approach was selected because of its flexibility and its capacity of managing several flows and equipment efficiently [15].

The system is made up of the following components: a PhotoVoltaic system (PV), a water ELectrolyzer (EL), an Electrical energy Storage System (EES), and a Hydrogen Storage tank (H2SS). In addition, a transformer was included to model the interface between the system and the power grid. The system is able to import electricity, water and hydrogen from an external source and export electricity and hydrogen to an external user.

The inputs to the energy hub are electricity purchased from the grid ( $E_{in}$ ), water needed to feed the electrolyzer ( $W_{in}$ ), and hydrogen transported by the tank trucks ( $H_{2 in}$ ).

The outputs of the system are the demands for electricity ( $E_{dem}$ ) and hydrogen ( $H_{2 dem}$ ), but also the electricity and hydrogen sold to an external user ( $E_{out}$  and  $H_{2 out}$ , respectively).

The optimization problem, based on mass balance and energy balance equations and energy flows, were solved in the MATLAB environment by resorting to a MILP algorithm [14,16].

The mathematical model illustrated in this section was conceived to be made up of linear equations, in order to ensure the uniqueness of the

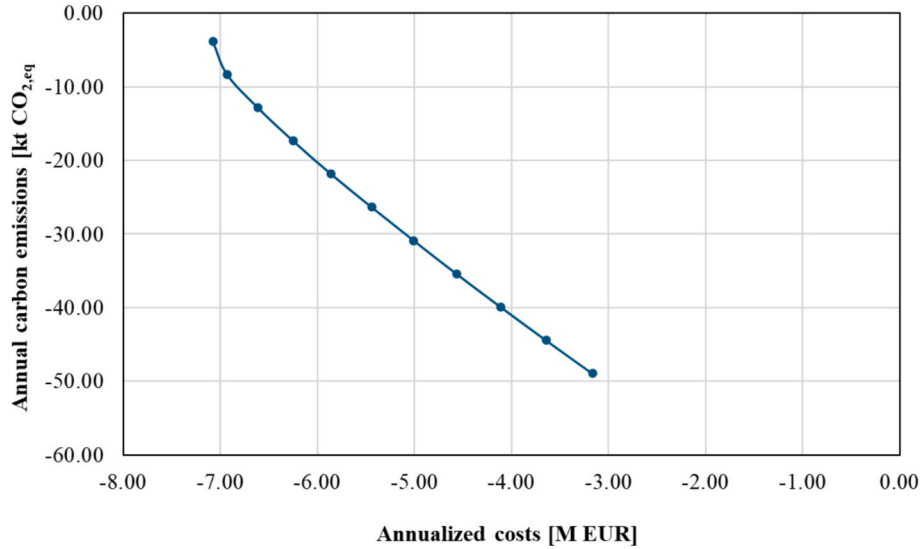


Fig. 7. Pareto front for the scenario 3.

Table 7

Optimal rated sizes, annualized costs and annualized carbon emissions for the dual-objectives optimization studies.

| Component   | Scenario 1    | Scenario 2           | Scenario 3           |
|---|---------------|----------------------|----------------------|
| PV system [MWp]   | 55.1          | 55.1                 | 55.1                 |
| EL [MW]   | 0             | 18.9                 | 9.6                  |
| EES [MWh]   | 0             | 0.0                  | 0.0                  |
| H2SS [ton H2]   | 8.2           | 8.2                  | 0.2                  |
| PV/EL ratio   | -             | 2.9                  | 5.7                  |
| <b>Annualized Costs [€]</b>                               | 2,076,140,699 | <b>676,168,529.6</b> | <b>-2,758,089.0</b>  |
| <b>Annualized Carbon Emissions [kg CO<sub>2,eq</sub>]</b> | 3,709,769,322 | <b>609,087,307.8</b> | <b>-32,639,333.1</b> |

Table 8

Ratio between the sizes of the PV system and the electrolyzer in the optimization studies.

| PV/EL RATIO                              | Scenario 1 | Scenario 2 | Scenario 3 |
|--|------------|------------|------------|
| Minimum Cost                             | -          | 1.85       | 2.03       |
| Minimum Carbon Emissions                 | -          | -          | -          |
| Dual-Objective minimization (on average) | -          | 2.91       | 5.75       |

optimal solution. The approximations deriving from the linearization of the behavior of the equipment were considered as limited due to the detailed modeling of the photovoltaic system and to the fact that large-scale water electrolyzers are actually modular equipment, thus a dependency of the efficiency from the load is considered as negligible.

## 2.2. Objective functions

The objective functions of the optimization problem, namely the annualized cost function and the annualized life cycle carbon dioxide emissions function, are shown in Eq. (1) and Eq. (2), respectively. The first objective function includes a first part, between brackets, related to operating terms, such as the costs and revenues for electricity, water, and hydrogen exchanges over the boundaries of the energy hub, and a second part related to the capital terms, assessing the purchase of equipment. The life-cycle emissions quantification is also based on the sum of operational terms, namely the life cycle carbon equivalent emissions related to the manufacture and supply of electricity, water, and hydrogen to the hub, and the capital terms, *i.e.* the embodied impact

in terms of carbon equivalent emissions for the manufacture, transportation, supply, replacement and dismission of each piece of equipment. For the assessment of the carbon emissions related to the equipment, the Global Warming Potential (GWP) per unit rated size was selected [17]. In Eq. (1), the investment terms were modelled using a unit size value,  $C_{capex}$ , depending on the rated size of the equipment  $S$ . For photovoltaic and electrolyzer systems, the rated size is the maximum power, while capacity was used for the storage systems.

In order to annualize these objective functions, the capital investment terms in Eq. (1) were multiplied by the Capital Recovery Factor (CRF) of each investment [18], while the embodied carbon of each equipment in Eq. (2) was divided for the useful life  $n$  of each equipment [16].

Due to convergency issues, the objective function was written considering  $K_{hour}$  operating hours per day and  $K_{day}$  operating days per year to be assessed, which can be then increased to the  $D_{year}$  effective number of annual days.

$$\min \frac{D_{year}}{K_{day}} \sum_{t=1}^{K_{day}K_{hour}} \{ C_{opex,E}E_{in}(t) + C_{opex,W}W_{in}(t) + C_{opex,H2}H_{2in}(t) - R_{opex,E}E_{out}(t) + R_{opex,H2}H_{2out}(t) \} + C_{capex,PV}CRF_{PV}S_{PV} + C_{capex,EES}CRF_{EES}S_{EES} + C_{capex,EL}CRF_{EL}S_{EL} + C_{capex,H2SS}CRF_{H2SS}S_{H2SS} \quad (1)$$

$$\min \frac{D_{year}}{K_{day}} \sum_{t=1}^{K_{day}K_{hour}} \{ GWP_E[E_{in}(t) - E_{out}(t)] + GWP_WW_{in}(t) + GWP_{H2}[H_{2in}(t) - H_{2out}(t)] \} + \frac{GWP_{PV}}{n_{PV}}S_{PV} + \frac{GWP_{EES}}{n_{EES}}S_{EES} + \frac{GWP_{EL}}{n_{EL}}S_{EL} + \frac{GWP_{H2SS}}{n_{H2SS}}S_{H2SS} \quad (2)$$

In the previous equations,  $C_{opex}$  and  $R_{opex}$  indicate operating costs and operating revenues, respectively, and are related to electricity (E), distilled water (W), and hydrogen (H2) flows, as indicated by their subscripts. Similarly,  $C_{capex}$ ,  $S$ ,  $n$  and  $CRF$ , explained above, are related to specific equipment, as indicated by their subscripts: Photovoltaic system (PV), Electrical Energy Storage (EES), Electrolyzer (EL), Hydrogen Storage System (H2SS). GWP indicates the embodied carbon emissions both for flows and equipment.

## 2.3. Constraints

The optimization problem formulated for this study is subject to

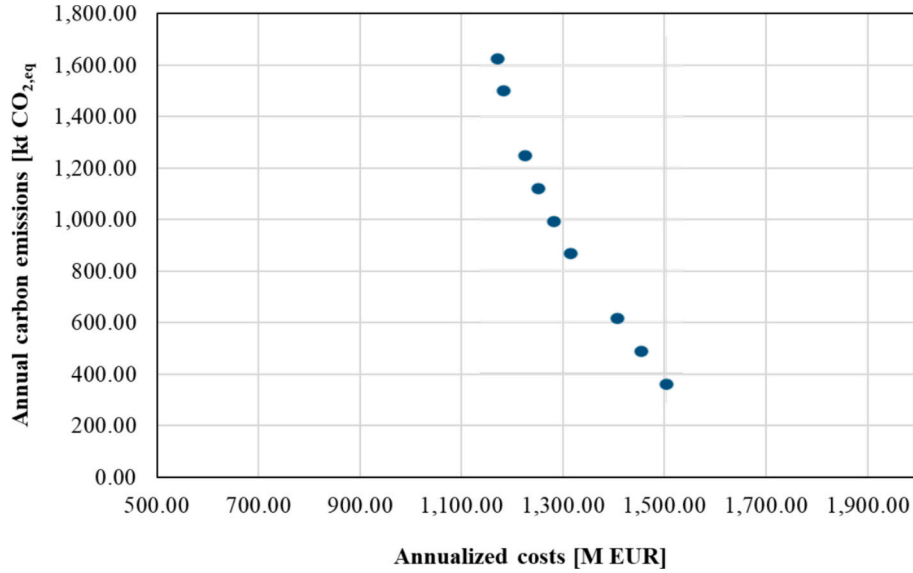


Fig. 8. Pareto front for the scenario 1 with increased PV area.

equality and inequality constraints included to describe the operation of the green hydrogen production plant.

Equality constraints involve the electricity flows balance, Eq. (3), the EES balance equation, Eq. (4), and the H2SS balance equation, Eq. (5). Additional constraints describe the behavior of the PV system, Eq. (6) [16], and set that the state of charge of the EES and H2SS at first and last timestep are the same, thus allowing the repeatability of the standard year (Eqn. (7) and (8)). It is important to highlight that this mathematical model might be easily extended to different renewable energies replacing Eq. (6) with different equations.

$$E_{in}(t)K_{TR} - E_{EES,ch}(t) + E_{EES,disch}(t) - E_{EL}(t) + E_{PV}(t) - E_{out}(t) = E_{dem}(t), \forall t \in T \quad (3)$$

$$SOC_{EES}(t+1) - SOC_{EES}(t)(1 - K_{EES,loss}) - E_{EES,ch}(t+1)K_{EES,ch} + \frac{E_{EES,disch}(t+1)}{K_{EES,disch}} = 0, \forall t \in T \quad (4)$$

$$SOC_{H2SS}(t+1) - SOC_{H2SS}(t)(1 - K_{H2SS,loss}) - [E_{EL}(t+1)K_{ELeh2} + H_{2in}(t+1)]K_{H2SS,ch} + [H_{2out}(t+1) + H_{2dem}(t+1)]/K_{H2SS,disch} = 0, \forall t \in T \quad (5)$$

$$E_{PV}(t) = A_{PV}K_{PV} \left\{ 1 + \beta_{PV} \left[ T_{air}(t) + \frac{I_{sun}(t)}{G_{NOCT}} (NOCT - T_{a,NOCT}) - T_{ref} \right] \right\} I_{sun}(t) S_{PV} / S_{PVm}, \forall t \in T \quad (6)$$

$$SOC_{EES}(0) - SOC_{EES}(T) = 0 \quad (7)$$

$$SOC_{H2SS}(0) - SOC_{H2SS}(T) = 0 \quad (8)$$

In the previous equations,  $K_{TR}$  is the efficiency of the transformer,  $E_{EES,ch}$  and  $E_{EES,disch}$  are respectively the electricity flows during the charge and discharge phases of the electrical storage,  $E_{EL}$  is the energy absorbed by the electrolyzer,  $E_{PV}$  is the energy coming from the photovoltaic system,  $SOC_{EES}$  and  $SOC_{H2SS}$  are the state of charge of the electric energy storage system and hydrogen storage system, respectively,  $K_{EES,loss}$  and  $K_{H2SS,loss}$  are coefficient used to quantify the self-

discharge losses in storage equipment,  $K_{EL} eh2$  is the electrolyzer electricity-to-hydrogen conversion rate,  $K_{EES,ch}$  and  $K_{EES,disch}$  are respectively the charge and discharge efficiencies of EES,  $K_{H2SS,ch}$  and  $K_{H2SS,disch}$  are respectively the charge and discharge efficiencies of H2SS accounting for leakages in pipelines,  $A_{PV}$  is the surface area of each PV module,  $K_{PV}$  is the PV radiation to electricity efficiency in standard conditions,  $\beta_{PV}$  is the PV cell temperature coefficient,  $T_{air}$  is the air temperature,  $I_{sun}$  is the solar irradiance of the selected location,  $G_{NOCT}$  is the reference solar radiance,  $NOCT$  is the PV nominal operating cell temperature,  $T_{a,NOCT}$  is the reference air temperature,  $T_{ref}$  is the reference cell temperature,  $S_{PV}$  is the size of photovoltaic plant, and  $S_{PVm}$  is the rated power of a single photovoltaic module.

In addition to the previous equations, inequality constraints were introduced for the management of storage systems and for linking the rated capacity of equipment to their operational variables. In detail, Eqn. (9)-(15) describe the operation of the electrical energy storage system, Eqn. (16)-(21) describe the operation of the hydrogen storage tank, and Eqn. (22)-(23) prevent the electrolyzer energy consumption and the photovoltaic energy production to overcome the rated size of these two components, respectively.

$$E_{EES,ch}(t) \leq \delta_{EES,ch}(t) S_{EES,max} \quad (9)$$

$$E_{EES,disch}(t) \leq \delta_{EES,disch}(t) S_{EES,max} \quad (10)$$

$$\delta_{EES,ch}(t) + \delta_{EES,disch}(t) \leq 1 \quad (11)$$

$$DoD_{EES} S_{EES} \leq SOC_{EES}(t) \quad (12)$$

$$SOC_{EES}(t) \leq S_{EES} \quad (13)$$

$$E_{EES,ch}(t) \leq S_{EES}(1 - DoD_{EES}) \quad (14)$$

$$E_{EES,disch}(t) \leq S_{EES}(1 - DoD_{EES}) \quad (15)$$

$$E_{EL}(t)K_{ELeh2} + H_{2in}(t) \leq S_{H2SS,max} \quad (16)$$

$$H_{2out}(t) + H_{2dem}(t) \leq S_{H2SS,max} \quad (17)$$

$$DoD_{H2SS} S_{H2SS} \leq SOC_{H2SS}(t) \quad (18)$$

$$SOC_{H2SS}(t) \leq S_{H2SS} \quad (19)$$

$$E_{EL}(t)K_{ELeh2} + H_{2in}(t) \leq S_{H2SS}(1 - DoD_{H2SS}) \quad (20)$$

$$H_{2out}(t) + H_{2dem}(t) \leq SH_{2SS}(1 - DoD_{H2SS}) \quad (21)$$

$$E_{EL}(t) \leq S_{EL} \quad (22)$$

$$E_{PV}(t) \leq S_{PV} \quad (23)$$

In the previous equations,  $\delta EES, ch(t)$  and  $\delta EES, disch(t)$  are Boolean variables used to prevent the battery from charging and discharging at the same time,  $SEES, max$  is the battery size upper limit,  $DoDEES$  is the battery depth of discharge,  $SEES$  is the rated capacity of the storage system,  $SH_{2SS}, max$  is the hydrogen tank size upper limit,  $DoDH_{2SS}$  is the depth of discharge of the hydrogen storage system and  $SH_{2SS}$  is its size, and  $SEL$  and  $SPV$  are the sizes of the electrolyzer and renewable power generation plant, respectively.

#### 2.4. Variables, bounds, and parameters

In the previous equations, main variables of the optimization model are the rated size for each equipment and the energy and mass flows related to each equipment and to main grid/network for each time step. Furthermore, storage systems are also characterized by a state of charge variable and two Boolean variables to state whether they are charging or discharging, for each time step. The optimization problem variables were collected in the vector  $\mathbf{x}$  whose entries can be real or Boolean values.

$$\mathbf{x} = [E_{in}(t), E_{EES, ch}(t), E_{EES, disch}(t), E_{EL}(t), E_{PV}(t), E_{out}(t), H_{2in}(t), H_{2out}(t), SOC_{EES}(t), SOC_{H2SS}(t),$$

$$\delta EES, ch(t), \delta EES, disch(t), S_{EES}, S_{H2SS}, S_{EL}, S_{PV} \quad (24)$$

Two additional vectors containing lower and upper bounds were defined for the different variables in the problem; in particular, the lower bounds were set equal to 0 for each variable, while the upper bounds are equal to infinity except for the Boolean variables, whose upper bounds are equal to 1, for the rated sizes of the storage systems, and for the size of the PV system  $SPV$ , which was limited according to the maximum area available in the industrial area.

Main parameters for the problem are the conversion efficiency terms for the equipment, final demands to be satisfied, costs and environmental impacts for the equipment and for the main grid/network. In addition, weather data (air temperature and solar radiation) were collected to evaluate the renewable electricity production.

#### 2.5. Multi-objective optimization

The multi-objective optimization problem (MOOP) in this study was solved using the  $\epsilon$ -constraint method, which allows solving a single-objective problem where one of the two objective functions is kept as main objective and the other one is converted into an additional inequality constraint of the problem [19]. In this study, the economic objective function shown in Eq. (1) was kept as objective function of the MOOP, while Eq. (2) was converted into a constraint. In order to identify the Pareto Front, namely the set of trade-off solutions of the MOOP, this constraint was alternatively set to be lower or equal to a set of values of equivalent carbon emissions belonging to the range between the following values:

- The minimum emissions of the system, obtained with the single-objective emission minimization;
- The emissions of the system allowing the minimum cost, obtained with the single-objective economic minimization.

### 3. Case study

The case study involves the industrial area surrounding a steel factory in Terni (Italy) with a steel production of 1,018,211 tons/year. The

local climate is quite mild, with an average annual temperature of 13 °C and an average annual solar radiation of 421 W/m<sup>2</sup>. This case study was selected because the steel production is among the *hard-to-abate* sectors and the introduction of green hydrogen in these companies might help in reducing their carbon footprint [20].

Main data regarding the factory steel production and energy use were gathered from the corporate sustainability report [21]. Due to the continuous operation of the plant, the cumulated demands were split over the year assuming 300 operating days and a flat demand over the hours of the day. Air temperature and solar radiation on the specific location from 2005 to 2023 were collected from the PVGIS database [22] and then averaged to create twelve monthly standard day. This aspect is a huge improvement with respect to the previous authors study [14], where a single standard day representative of the whole year was simulated.

Last, the green hydrogen production system (PV + electrolyzer + tank) was supposed to operate for 360 days/year, assuming 5 days/year for maintenance.

For the case study, the electrical energy storage system technology was assumed as a li-ions battery system. Thus, although the mathematical modelling generically refers to any technology, costs and impacts were selected for this kind of technology.

In order to enrich the study, starting from the data described above, three sets of optimization studies were run, considering the following demand profiles, keeping constant the other aspects:

- **Scenario 1:** industrial site with electricity and hydrogen demands, i.e. the steel factory;
- **Scenario 2:** industrial site with hydrogen demand only ( $E_{dem} = 0$ ), such as the steel factory using only electricity from the grid or another large facility with negligible or limited electricity demand, such as an oil refinery;
- **Scenario 3:** industrial site without demands ( $E_{dem} = H_{2dem} = 0$ ), such as a plant intended for the production and sale of green electricity and green hydrogen.

The main data used to describe the case study are shown in Table 2, Table 3, and Table 4. In detail, the values of the coefficients for the cost function are given in Table 2, the values of the coefficients for the emissions function are given in Table 3, while the values of the additional technical parameters such as components' efficiencies are listed in Table 4.

## 4. Results

#### 4.1. Economic Minimization

Table 5 shows the results obtained minimizing the annualized costs in the three case studies assessed in this article, in terms of components' rated sizes, annualized costs and annualized carbon emissions. In these studies, it is evident that the optimal PV rated size is constant and is equal to the upper bound allowed to the optimization study, related to the maximum area available. Accordingly, the rated sizes of the other components and the objective functions are determined by the algorithm, with a ratio close to 2 in scenario 2 and 3, while the electrolyzer is not installed in the scenario 1 since the supply from an external provider is economically more convenient. All these scenarios also include the installation of a hydrogen storage tank, in order to store the hydrogen coming from the external provider or the excess hydrogen production when the solar radiation is high. Regarding the objective functions, results are very different since the applications are very different. In detail, since the installation of green hydrogen production plant is constrained by the availability of enough area, its contribution to the final demands is limited. This causes a huge reduction from the first scenario to the second, where there is no electricity demand, while the third case has negative values, since selling green electricity and green hydrogen

greatly overcomes the capital costs for the installation of the equipment.

Regarding the management schedules, the very high values of demands force the algorithm to resort on external sources both for electricity and hydrogen supply, since the complete self-consumption from renewables would require huge values of rated sizes. An example of electricity and hydrogen daily trends over the three scenarios is provided in Fig. 2 and Fig. 3, respectively, while additional results are provided in the Supporting Information.

#### 4.2. Emissions Minimization

Table 6 shows the results obtained minimizing the annualized carbon equivalent emissions in the three case studies assessed in this article, in terms of components' rated sizes, annualized costs and annualized carbon emissions. Similarly to the previous case, the optimal PV rated size is constant among the three studies and is equal to the maximum area available, confirming that PV is both a cost-effective and carbon-effective technology. Nevertheless, the low value set for the embodied carbon in the green hydrogen coming from the external supplier drives the optimization algorithm to disregard the installation of the water electrolyzer. It is worth to highlight that this result might be strongly related to the specific climatic conditions, since repeating the simulations in a sunnier location might change these results. Regarding scenario 1, it is interesting noting that the annualized carbon emissions are the same with respect to the minimum cost scenario. Regarding scenario 3, minimizing carbon emissions drives the optimization to set all the hydrogen flows equal to zero and injecting all the renewable electricity into the grid.

Regarding the management schedules, the very high values of demands force the algorithm to resort on external sources both for electricity and hydrogen supply even in emissions minimal cases. An example of electricity and hydrogen daily trends over the three scenarios is provided in Fig. 4 and Fig. 5, respectively, while additional results are provided in the Supporting Information.

#### 4.3. Dual-objective minimization

In addition to the six optimization studies described above, several additional cases were investigated to find intermediate optimal solutions balancing economic and environmental aspects. These trade-off solutions, known as non-dominated solutions, make up the Pareto Front of the MOOP. Fig. 6 shows the Pareto Front for the scenario 2, while Fig. 7 shows the Pareto Front for the scenario 3. Scenario 1 was not represented since all the solutions were very close to each other, since minimizing annualized costs also allows minimizing emissions. The average values of components' rated sizes, annualized costs and annualized carbon emissions are shown in Table 7, where intermediate results with respect to the previous two sets of optimization studies can be easily identified.

#### 4.4. Discussion

From the results shown in Fig. 6 and Fig. 7, the cost-optimal ratio between the sizes of the PV system and the electrolyzer is between 1.83 and 2.04, depending on the scenario, and between 2.89 and 5.5 when a trade-off between minimizing costs and minimizing carbon dioxide emissions is to be achieved. A recap of the solutions is provided in Table 8.

In addition, since the results for scenario 1 always drive to disregard the installation of electrolyzers, the authors further investigated this case. In detail, the authors remarked that optimization results were heavily influenced by the value imposed for maximum PV area, considering that the value of PV installed power was always equal to the upper bound.

For this reason, additional simulations were run imposing that the available area was increased to 60 times higher. In this way, the

renewable production was able to cover about the 83 % of the annual electricity demand, rather than only 2 % as in the previous cases. With these conditions, a proper Pareto Front was built, as illustrated in Fig. 8. In these cases, the PV/EL size ratio was equal to 5.4, on average.

## 5. Conclusions

In the current decarbonization process, developing quick and useful tools to improve the integration of renewable energies and hydrogen as a new vector is mandatory. This study illustrated the development of a MILP optimization model designed to optimize the configuration of an energy hub integrating PV energy generation and hydrogen production via electrolysis. Although the topic of green hydrogen production is being assessed extensively in the last few years, a criterion for sizing the electrolyzer with respect to the PV nominal power is still not available in the international literature, to the best of authors' knowledge. The primary objective was to determine the optimal size ratio between the PV system and the electrolyzer to maximize efficiency under varying operational and demand constraints. To assess the model's applicability across different industrial contexts, three distinct scenarios were evaluated, involving hydrogen production from stand-alone plant, production to meet final hydrogen demand, and simultaneous hydrogen and electricity production to meet both demands. Each scenario was analyzed from both economic and environmental perspectives, minimizing the annualized costs or the annual carbon equivalent emissions, thus providing a comprehensive assessment of system performance under different operational strategies.

The optimization results revealed that the cost-minimized PV-to-electrolyzer capacity ratio falls within the range of 1.8 to 2, which aligns with findings from previous studies focused on dedicated green hydrogen plants without additional energy demands. This ratio ensures that the electrolyzer operates near its maximum efficiency while avoiding excessive PV curtailment during peak production periods. However, when environmental impact minimization was included as an additional objective, the optimal ratio increased significantly—reaching up to 5.75—reflecting the need for oversized PV capacity to maximize renewable energy utilization and minimize reliance on grid electricity (which may have a higher carbon footprint). This highlights a critical trade-off between cost efficiency and carbon reduction, suggesting that policy incentives or carbon pricing mechanisms could influence the optimal system design in real-world applications.

The results obtained for this study are influenced by the technologies selection, namely a PV system for renewable energy generation and a battery system for electrical storage. It is reasonable to assume that the optimal solutions might change with different technologies, especially with reference to the storage system, since pumped hydro or hydrogen-based electricity storage have different performance. Nevertheless, these technologies are the most commonly used and versatile currently available. Furthermore, although this article has addressed the case study of three industrial contexts, the mathematical model presented is a generic model that lends itself to various applications, including residential ones.

Further developments of this study might involve evaluating the integration of different renewable energy sources in lieu of photovoltaic, such as wind or hydropower, as well as considering hybrid renewable plants. In addition, an uncertainty analysis on the availability of renewable energy might be assessed resorting to a Monte Carlo algorithm. Last, the study might be repeated considering different values of final demands and different climatic conditions.

#### CRediT authorship contribution statement

**Francesco Guarino:** Writing – review & editing, Methodology, Funding acquisition. **Angelo Gucciardi:** Writing – review & editing, Writing – original draft, Visualization, Software, Investigation, Formal analysis, Conceptualization. **Fabio Massaro:** Writing – review &

editing, Methodology, Funding acquisition, Formal analysis, Conceptualization. **Francesco Montana**: Writing – review & editing, Writing – original draft, Methodology, Investigation, Formal analysis, Data curation, Conceptualization. **Salvatore Ruffino**: Writing – review & editing, Writing – original draft, Visualization, Software, Investigation, Formal analysis, Data curation, Conceptualization.

### Declaration of competing interest

The authors declare that they have no known competing financial interests or personal relationships that could have appeared to influence the work reported in this paper.

### Appendix A. Supplementary data

Supplementary data to this article can be found online at <https://doi.org/10.1016/j.ref.2025.100744>.

### Data availability

Data will be made available on request.

### References

- [1] M.R. Usman, "Hydrogen storage methods: review and current status," 2022. doi: 10.1016/j.rser.2022.112743.
- [2] International Energy Agency (IEA), "Renewables 2024," 2024. Accessed: Oct. 16, 2024. [Online]. Available: <https://www.iea.org/reports/renewables-2024>.
- [3] International Energy Agency (IEA), "Global Hydrogen Review 2024," 2024. Accessed: Oct. 16, 2024. [Online]. Available: <https://www.iea.org/report-s/global-hydrogen-review-2024>.
- [4] Institute of Climate and Energy Systems (ICE), "ETHOS Model Suite." Accessed: Oct. 17, 2024. [Online]. Available: <https://www.fz-juelich.de/en/ice/ice-2/expertise/model-services>.
- [5] M. Ferraro, F. Massaro, E. R. Sanseverino, S. Ruffino, "Is Selling the Oxygen Produced During Electrolysis Really a Solution to Make Green Hydrogen Cheaper?," in *2024 IEEE International Conference on Environment and Electrical Engineering and 2024 IEEE Industrial and Commercial Power Systems Europe (EEEIC / I&CPS Europe)*, 2024, pp. 1–6. 10.1109/EEEIC/ICPSEurope61470.2024.10751545.
- [6] H. Tebibel, Methodology for multi-objective optimization of wind turbine/battery/electrolyzer system for decentralized clean hydrogen production using an adapted power management strategy for low wind speed conditions, *Energy Convers. Manage.* 238 (2021), <https://doi.org/10.1016/j.enconman.2021.114125>.
- [7] A.X.Y. Mah, et al., Optimization of a standalone photovoltaic-based microgrid with electrical and hydrogen loads, *Energy* 235 (2021), <https://doi.org/10.1016/j.energy.2021.121218>.
- [8] F. Massaro, M. Ferraro, F. Montana, E. Riva Sanseverino, S. Ruffino, Techno-economic analysis of clean hydrogen production plants in sicily: comparison of distributed and centralized production, *Energies* 17 (13) (2024), <https://doi.org/10.3390/en17133239>.
- [9] M.M. Hasan, G. Genç, Techno-economic analysis of solar/wind power based hydrogen production, *Fuel* 324 (2022) 124564, <https://doi.org/10.1016/j.fuel.2022.124564>.
- [10] Y. Astriani, W. Tushar, M. Nadarajah, Optimal planning of renewable energy park for green hydrogen production using detailed cost and efficiency curves of PEM electrolyzer, *Int. J. Hydrogen Energy* 79 (2024) 1331–1346, <https://doi.org/10.1016/J.IJHYDENE.2024.07.107>.
- [11] M. Al-Mahmodi, O. Ayadi, Y. Wang, A. Al-Halhouli, Sensitivity-based techno-economic assessment approach for electrolyzer integration with hybrid photovoltaic-wind plants for green hydrogen production, *Int. J. Hydrogen Energy* 97 (2025) 904–919, <https://doi.org/10.1016/J.IJHYDENE.2024.12.002>.
- [12] A. González del Valle, P. García-Linares, A. Martí, Optimizing hydrogen Production: a comparative study of direct and indirect coupling between photovoltaics and electrolyzer, *Energy Convers. Manage.* 315 (2024) 118751, <https://doi.org/10.1016/J.ENCONMAN.2024.118751>.
- [13] P. Martorana, M. Mantegna, V. Frazitta, M.A. Judge, M. Franzitta, V. Vitrano, Optimization of a PTO for wave energy harvesting on breakwaters, *Oceans Conf. Rec. (IEEE)* (2024), <https://doi.org/10.1109/OCEANS51537.2024.10682360>.
- [14] M. Coveri et al., "Economic Optimization of the Hydrogen Demand in a Hard-to-Abate Industrial Sector," in *Conference Proceedings - 2023 IEEE Asia Meeting on Environment and Electrical Engineering, EEE-AM 2023*, 2023. 10.1109/EEE-AM58328.2023.10395195.
- [15] M. Geidl, G. Koeppel, P. Favre-Perrod, B. Klöckl, G. Andersson, K. Fröhlich, "The Energy Hub – A Powerful Concept for Future Energy Systems," 2007.
- [16] F. Massaro, M.L. Di Silvestre, M. Ferraro, F. Montana, E. Riva Sanseverino, S. Ruffino, Energy hub model for the massive adoption of hydrogen in power systems, *Energies (Basel)* 17 (17) (2024), <https://doi.org/10.3390/en17174422>.
- [17] F. Guarino, M. Cellura, M. Traverso, Constructal law, exergy analysis and life cycle energy sustainability assessment: an expanded framework applied to a boiler, *Int. J. Life Cycle Assess.* 25 (10) (2020) 2063–2085, <https://doi.org/10.1007/s11367-020-01779-9>.
- [18] W. Short, D.J. Packey, T. Holt, "A Manual for the Economic Evaluation of Energy Efficiency and Renewable Energy Technologies," 1995.
- [19] G. Mavrotas, Effective implementation of the  $\epsilon$ -constraint method in multi-objective mathematical programming problems, *Appl. Math. Comput.* 213 (2) (2009) 455–465, <https://doi.org/10.1016/J.AMC.2009.03.037>.
- [20] M.L. Di Silvestre, M.G. Ippolito, F. Massaro, F. Montana, E.R. Sanseverino, S. Ruffino, "Hydrogen Utilization in Industry. A Cost Comparison between On-Site Production and External Supply," *Conference Proceedings - 2023 IEEE Asia Meeting on Environment and Electrical Engineering, EEE-AM 2023*, 2023. 10.1109/EEE-AM58328.2023.10395828.
- [21] Acciai Speciali Terni, "Bilancio sostenibilità 2019," 2019.
- [22] "Photovoltaic Geographical Information System (PVGIS) - European Commission." Accessed: Nov. 28, 2024. [Online]. Available: [https://joint-research-centre.ec.europa.eu/photovoltaic-geographical-information-system-pvgis\\_en](https://joint-research-centre.ec.europa.eu/photovoltaic-geographical-information-system-pvgis_en).
- [23] "Database - Eurostat." Accessed: Nov. 28, 2024. [Online]. Available: <https://ec.europa.eu/eurostat/web/main/data/database>.
- [24] Autorità di Regolazione per Energia Reti e Ambiente (ARERA), *Ritiro dedicato e prezzi minimi garantiti*. 2024. Accessed: Apr. 07, 2025. [Online]. Available: <https://www.arera.it/elettrica/ritiro-dedicato-e-prezzi-minimi-garantiti>.
- [25] International Renewable Energy Agency (IRENA), "Renewable Power Generation Costs in 2023," Abu Dhabi, 2024.
- [26] IEA, "Projected Costs of Generating Electricity," 2020.
- [27] ARERA, "Deliberazione 28 novembre 2023, 556/2023/R/COM," 2023. Accessed: Nov. 28, 2024. [Online]. Available: <https://www.arera.it/fileadmin/allegati/docs/23/556-23.pdf>.
- [28] "European Platform on LCA|EPLCA." Accessed: Nov. 28, 2024. [Online]. Available: <https://eplca.jrc.ec.europa.eu/ELCD3/>.
- [29] S. Di Carlo, A. Genna, F. Massaro, F. Montana, E.R. Sanseverino, "Optimizing Renewable Power Management in Transmission Congestion. An Energy Hub Model Using Hydrogen Storage," in *21st IEEE International Conference on Environment and Electrical Engineering and 2021 5th IEEE Industrial and Commercial Power System Europe, EEEIC/I and CPS Europe 2021 - Proceedings*, Institute of Electrical and Electronics Engineers Inc., 2021. 10.1109/EEEIC/ICPSEurope51590.2021.9584510.